Raman spectra of a high-pressure iodine single crystal

A. Congeduti and P. Postorino
Dipartimento di Fisica, Università di Roma "La Sapienza," Unita' dell'Istituto Nazionale di Fisica per la Materia, Piazzale A. Moro 2, 00185 Roma, Italy

M. Nardone
Dipartimento di Fisica, Università di Roma Tre, Unita' dell'Istituto Nazionale di Fisica per la Materia, Via della Vasca Navale 84, 00146 Roma, Italy

U. Buontempo
Dipartimento di Fisica, Università dell'Aquila, Unita' dell'Istituto Nazionale di Fisica per la Materia, Via Vetoio, 67010 L' Aquila, Italy

(Received 12 April 2001; published 29 November 2001)

Raman spectra have been collected in iodine single crystal at room temperature in the pressure range 1–14 GPa using a micro-Raman apparatus. The pressure at the sample was generated by means of a diamond anvil cell. Single crystals were grown *in situ* over the inner diamond surface. A careful analysis of the frequencies and intensities of internal (stretching) and external (libration) modes as a function of the pressure is reported. In particular, analysis of the relative intensities of the Raman modes confirms a theoretical prediction about the pressure evolution of the A_g stretching mode eigenvector and the huge intensity increase of the external modes with respect to the internal ones is well consistent with the predicted increased role of the charge-transfer interaction when approaching the metallization transition pressure. At pressures higher than 10 GPa, spectral features were observed simultaneously with the appearance of two peaks forbidden in the adopted sample geometry. The experimental results obtained are eventually discussed in comparison with recent experimental and theoretical works.

DOI: 10.1103/PhysRevB.65.014302 PACS number(s): 62.50.+p, 71.30.+h, 78.30.−j

I. INTRODUCTION

One of the most intriguing phenomena exhibited by matter under extreme pressure conditions is the occurrence of the metallization transition. It is well known that diatomic molecular systems show a metallic behavior when the distances between nonbonded atoms become comparable with the molecular bond length. Even though the exact path from the molecular nonmetal to the atomic metal is often not well defined from both an experimental and theoretical point of view, a two-step transition is nowadays predicted for a variety of systems: a first nonmetal-to-metal transition, which preserves the molecular unit, followed by a transition from a molecular-metallic phase to an atomic-metallic phase. The metallic and dissociation transition pressures depend upon the peculiar characteristics of the system. In particular low transition pressures are found for systems with small energy gap and high intermolecular interaction.

Iodine is an ideal system for studying the evolution from an insulating molecular system towards the high-pressure atomic metal. Under ambient conditions, iodine is a semiconductor[1] with an energy gap of 1.35 eV and many of the properties of its condensed phases are driven by the strong intermolecular interaction.[2–6] The iodine crystal belongs to the face-centered orthorhombic $Cmca$ (D_{2h}^{18}) space group ($a=7.136$ Å, $b=4.686$ Å, and $c=9.784$ Å at $P=0$). The molecules lie in the bc plane in a zigzag planar arrangement stacked along the a axis.[7,8] The distance between first neighboring atoms (3.49 Å) is shorter than twice the van der Waals radius ($2R_{vW}=4.15$ Å) and suggests a remarkable intermolecular interaction.[9] At room temperature, the metallization transition was observed in the molecular phase at 16 GPa and ascribed to a band overlap mechanism.[1] The crystal structure remains unchanged up to 21 GPa where the dissociation transition takes place with a structural transition to a monatomic orthorhombic bco structure [$Immm(D_{2h}^{25})$].[10,11] The dependence of the structure on the applied pressure is well known from x-ray diffraction experiments:[9,12] the unit cell contracts anisotropically ($\Delta a/a > \Delta b/b > \Delta c/c$), reaching a volume compression of more than 30% at 21 GPa. The molecular axis, forming an angle γ of about 32° with the long axis c at ambient pressure, rotates and the γ value increases up to ~40° in the molecular metallic phase. These large changes in the crystal structure induce a small increase of the intramolecular distance (from 2.720 Å at $P=0$ to 2.740 Å at $P=6$ GPa).[9,13] As a matter of fact, a strong pressure-driven intermolecular interaction modifies the intramolecular potential in a way to approximately balance the lattice compression.[14] Electron density maps, obtained by an advanced x-ray diffraction data analysis, show a systematic increase of the electronic delocalization in the bc plane as the pressure is increased.[15] The appearance at high pressure of a planar network of strongly connected molecules (zigzag chains) in qualitative agreement with the theoretical calculation[16] has been regarded as a precursor of the insulator-to-metal transition.

Changes in the polarizability are expected to be induced by this electronic rearrangement and therefore Raman spectroscopy is an ideal tool to probe them. In the orthorhombic phase the internal stretching modes ($A_g^{(S)}$ and $B_{3g}^{(S)}$) are both Raman active while only four external modes (B_{1g}, B_{2g},

$A_g^{(L)}$, and $B_{3g}^{(L)}$ librations) are Raman active.[17,18] High-pressure Raman studies have been also carried out on iodine[19,20] up to 27 GPa. In agreement with lattice dynamics calculations performed using a rather complex potential model,[21] a weak pressure dependence of the internal modes in comparison with that shown by the external ones was observed up to the molecular-atomic transition where all the spectral features disappear.[19,20] The spectra collected at pressures above 10 GPa showed the appearance of spectral features which were discussed with respect to the onset of a quasi-one-dimensional molecular network in the bc plane (i.e., the zigzag chain above mentioned).[20] A simple bond charge model has also been proposed to account for the results from Raman and x-ray diffraction high-pressure data.[14,22] Within this model the observed pressure dependence of the phonon modes has been mainly ascribed to remarkable changes in the relative distribution of the bond charge and in particular to the increase of the two intermolecular bond charges with respect to the intramolecular one.[14,22,23] Unfortunately, due to the polycrystalline nature of the samples, no intensity analysis was reported in the previous high-pressure papers.[19,20] This analysis would be of great interest since the intensity of the Raman peaks is related to the charge density involved in the phonon modes and can therefore be useful in investigating the occurrence of charge transfer processes. As a matter of fact a polarization analysis of Raman intensities collected at ambient condition has shown the presence of a detectable charge transfer from within the molecule towards the intermolecular bonding region.[18]

In this paper we report an analysis of Raman spectra collected on a single crystal of iodine in the 1–14 GPa pressure range. The experiment was performed using a diamond anvil cell for generating the pressure and a micro-Raman setup for collecting the spectra. Iodine single crystals were grown *in situ* on the diamond surface. This procedure in conjunction with the high quality of the data allowed us to study the pressure dependence of the intensity of the allowed Raman modes.

II. EXPERIMENT

Raman spectra were collected by means of a LABRAM spectrometer (by Dilor) using a 632.8-nm excitation from a 16-mW He-Ne laser. A confocal microscope focused the polarized laser beam and provided collection of backscattered photons. An optical notch filter is used to improve rejection of the elastically scattered light from sample and optics. A polarization analyzer is used to select the polarization of the scattered light. A 30-cm-focal-length grating monochromator disperses the spectra on a cooled low-noise 1024×256 pixel charge-coupled device (CCD). In the present experiment, a 22-mm-focal-length ($20\times$magnification) objective was used and the confocal pinhole was adjusted to obtain a scattering volume of only a few μm across. The entrance slit of the monochromator was set to yield the ultimate resolution of the instrument which was better then 3 cm^{-1} in the spectral region investigated. By slightly tilting the notch filter, we were able to collect reliable spectra down to 80 cm^{-1}. Finally, an absolute frequency calibration was performed using the known emission lines from a Ne lamp.

High pressure at the sample was generated by a membrane diamond anvil cell (MDAC) purchased by BETSA. The anvils were low-fluorescence II A diamonds with an 800-μm culet diameter; the gaskets, 250 μm thick, were made of a Mo foil in order to withstand chemical reactions of iodine. Under working conditions the sample inside the gasket had a typical diameter of 300 μm and was 30–50 μm thick. The pressure on the sample was measured after each Raman acquisition on I_2 by collecting the fluorescence spectrum from small ruby chips placed at the surface of the sample itself.[24] The pressure uncertainties were estimated to be ±0.1 GPa.

The sample, doubly sublimated I_2 powder (by Mercks), was always handled with ceramic tools in a glove box maintained a low temperature (below 5 °C) under N_2 atmosphere in order to prevent chemical contamination. A pellet was obtained by synthesizing I_2 fine powder at high pressure in the gasket hole. After heating up the cell to room temperature, the load on the diamond anvils was released and a small quantity of iodine was allowed to sublimate outside the cell. After resealing the cell by applying the load on the anvils, we obtained a gasket hole partially filled with I_2. Finally, by impulsive laser heating of the surface of the sample, we were able to grow by sublimation small single crystals on the inner free surface of the diamond. The pressure on the single crystals was generated by a further increase of the load on the anvils. Due to the complexity of loading the sample, no pressure transmitting media were used as well as in Ref. 20. The lowest pressure attained following this procedure was around 1 GPa. Crystals grown in the MDAC were identified by means of a microscope under polarized light since differently oriented crystalline domains appear as different gray tones. We want to note that, because of the very high thermal conductivity of diamond, crystals grown directly on diamond do not suffer any detectable increase of temperature caused by the laser beam. The absence of laser heating on the sample was checked by analyzing the Stokes/antiStokes ratio.[18] The crystals grow with the bc plane parallel to the diamond surface (as reported also in Ref. 25). In this geometry, the electric field of the incoming laser beam lies in the bc plane and therefore the only allowed modes are those of A_g and B_{3g} symmetry, namely two internal (stretching) and two external (librational) modes. The quality and orientation of the crystals were also checked by collecting Raman spectra at the lowest pressure on different crystalline domains with parallel polarization configuration (i.e., with the polarization axes of the analyzer parallel to that of incoming laser beam). In Fig. 1 the spectra from the darkest and lightest domains are shown in the frequency range of the vibrational modes. In the former (the ''dark gray'' one) both A_g and B_{3g} vibrational modes are well evident while in the latter (the ''light gray'' one) the B_{3g} mode has practically disappeared. From the intensity ratio of the two modes, according to the previously reported polarization analysis,[18] we can infer that the electric field of the incoming laser beam makes an angle θ greater than 60° with the b axis for the dark gray crystal

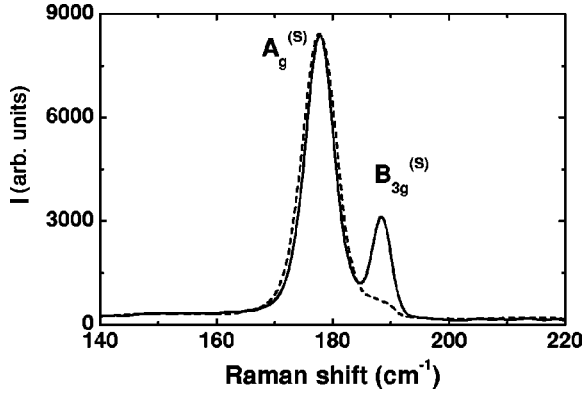

FIG. 1. Raman spectra of iodine collected at $P=0.9$ GPa focalizing on a ''dark gray'' (solid line) and on a ''light gray'' (dashed line) crystal. The absence of the $B_{3g}^{(S)}$ mode in the spectrum from light gray crystal confirms the very good crystallinity and the different orientation of the two crystals (see Ref. 18).

while it is almost parallel to the *b* axis for the light gray crystal.

We collected Raman spectra with parallel polarization as a function of pressure in the 1–14 GPa range from the darkest domain owing to the low Raman intensity from the lighter domains. A systematic reduction of the overall Raman signal was observed as the pressure was increased but a quantitative analysis of this effect was not attempted due to the strong dependence of the Raman intensity on focusing. As a matter of fact, after each increase of pressure we adjusted the distance of the objective for optimizing the intensity of the Raman signal. We want to point out that the absolute intensities of the Raman modes can be affected by both different focusing and optical properties which can show a pressure dependence (e.g., the refraction index). In the following, therefore, we just deal with the pressure dependence of intensity ratios between Raman modes, these quantities being not affected by variation of the absolute intensity of the Raman signal.

In Fig. 2 the spectrum collected at 5 GPa is shown. Lattice librational ($A_g^{(L)}$ and $B_{3g}^{(L)}$) and molecular stretching

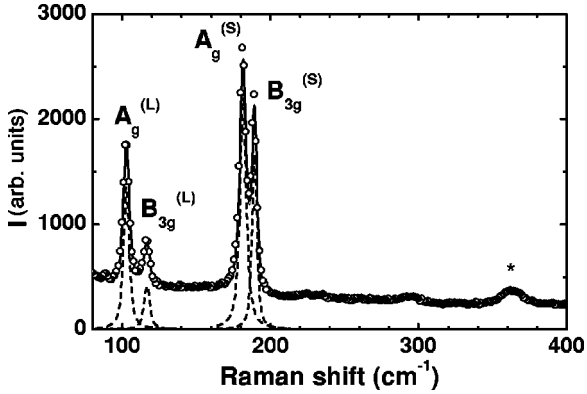

FIG. 2. Raman spectrum of iodine at $P=5$ GPa; the solid line is the best-fit curve obtained by four Voigt profiles plus a low-order polynomial background. The asterisk marks the position of the first overtone of the vibrational modes.

($A_g^{(S)}$ and $B_{3g}^{(S)}$) modes, centered at 101 cm^{-1}, 113 cm^{-1}, 182 cm^{-1}, and 191 cm^{-1}, respectively, are quite intense and well resolved. Minor broad structures are also detectable around 225 cm^{-1}, 290 cm^{-1}, and 370 cm^{-1}. The latter, marked by an asterisk in Fig. 2, can be safely ascribed to the first overtone of the stretching modes while the others are stretching-libration combination bands. In the following we will focus on the pressure dependence of the A_g and B_{3g} one-phonon peaks.

The high quality of the data, together with the *in situ* crystal growth technique and the high spatial resolution of the confocal microscope, allowed us to perform a careful shape analysis of the Raman peaks. The central frequency, the widths, and the integrated intensities of internal and external modes were determined by fitting the experimental data with Voigt profiles in the stretching and librational frequency range. A typical best-fit curve together with the four single-phonon contributions is also shown in Fig. 2. A low-power polynomial background was also used in the fitting routine. Very good agreement between the experimental data and the fitting curve shown in Fig. 2 was obtained for all the spectra at the different pressures.

III. RESULTS AND DISCUSSION

In Fig. 3(a) room-temperature Raman spectral intensities (I) from solid iodine at different pressures P are shown in a (ν,P) three-dimensional plot. Photon counts were normalized to the integrated intensity of the $A_g^{(S)}$ stretching mode. In Fig. 3(b) a smoothed intensity plot in gray tones of I on the (ν,P) plane is shown. The main four peaks are the two librational modes and the two molecular stretching modes in the 80–120 cm^{-1} and 180–210 cm^{-1} frequency ranges, respectively. The pressure-induced hardening of all these modes is well evident in the 1–10 GPa range, albeit less pronounced for the internal modes. A saturation in the pressure dependence of the librational mode frequencies and the crossing of the internal $A_g^{(S)}$ and $B_{3g}^{(S)}$ modes in the 10 GPa pressure range are also evident in Fig. 3(b). Our data are in good agrement with the pressure dependence of the experimental frequencies reported in Ref. 20 and shown in Fig. 3(b) as white circles. The pressure dependences are also in agreement with theoretical calculations.[21]

The most relevant feature that clearly emerges from Figs. 3(a) and 3(b) is the remarkable pressure dependence of the Raman peak intensities. In particular, the spectra show a dramatic increase of the librational mode intensities with respect to the vibrational ones. Although, as mentioned above, a comparison among the absolute intensities between different spectra may be questionable, a detailed analysis of peak intensity ratios can be safely performed for each spectrum. The best-fit values obtained for the integrated intensities of stretching and librational modes was used in the intensity analysis. The pressure dependence of the intensity ratio $A_g^{(S)}/B_{3g}^{(S)}$ is shown in Fig. 4, and the ratios between the intensities of librational and stretching modes having the same symmetry ($A_g^{(L)}/A_g^{(S)}$ and $B_{3g}^{(L)}/B_{3g}^{(S)}$) are shown on a logarithmic scale in Fig. 5. Up to about 10 GPa all the reported

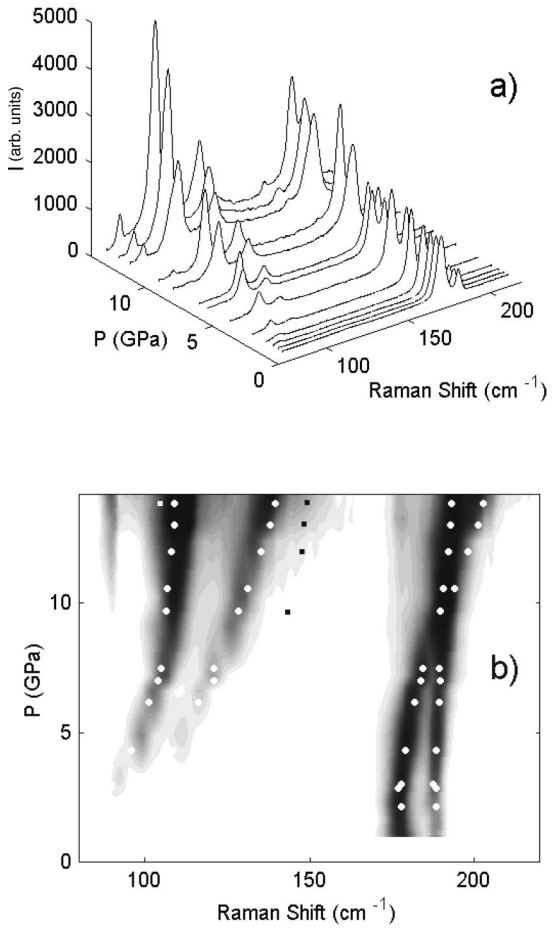

FIG. 3. (a) Three-dimensional plot of room-temperature Raman spectra as a function of pressure. Each spectrum was normalized to the integrated intensity of the $A_g^{(S)}$ stretching mode. (b) Smoothed intensity plot in grey tones as a function of pressure and frequency (the higher the intensity, the darker the tone). White circles are the measured peak frequencies reported in Ref. 20 for the internal and external A_g and B_{3g} modes. White and black squares are the frequencies measured in Ref. 20 for the X and Y structures, respectively.

pressure dependences show a quite regular and monotonic behavior, giving us further confidence about both crystal and alignment stability. In particular, as the pressure is increased, the intensity values of the two stretching modes become very similar (see Fig. 4) and a huge increase of the librational/stretching ratios takes place (see Fig. 5). The increase of about two orders of magnitude in the intensity ratios $A_g^{(L)}/A_g^{(S)}$ and $B_{3g}^{(L)}/B_{3g}^{(S)}$ can be well reproduced, in the 1–10 GPa pressure range, by an exponential growth (dashed and solid lines in Fig. 5). At pressures greater than 10 GPa the data shown in Figs. 4 and 5 scatter away from the described trend, suggesting that something is occurring to the sample. In this same high-pressure regime two new small peaks appear in the spectra at around 90 cm^{-1} and 125 cm^{-1}, as can be seen by an inspection of both Figs. 3(a) and 3(b). In Fig. 6 a single spectrum collected at $P=14$ GPa is shown where the new peaks are marked by arrows. Based on the theoretical prediction for the phonon frequencies pressure

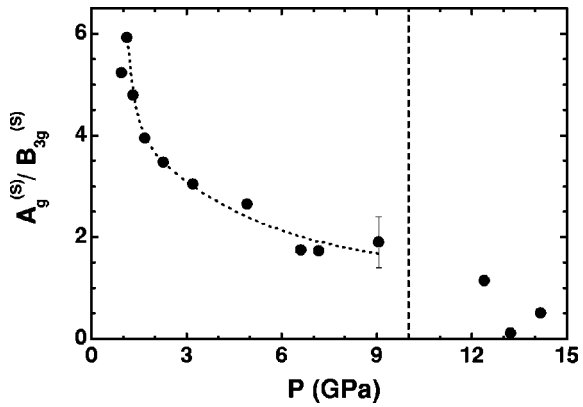

FIG. 4. Integrated intensity ratio $A_g^{(S)}/B_{3g}^{(S)}$ between the stretching modes as a function of pressure. The dotted line is a guide for the eyes; the dashed vertical line indicates the pressure at which crystal damage occurs. The 9 GPa ratio is affected by a large uncertainty since the two peaks are almost superimposed.

evolution[21] these peaks can be tentatively ascribed to the B_{2g} mode (90 cm^{-1}) and to the first overtone of the B_{1g} (125 cm^{-1}) mode, which are both forbidden in the original sample geometry. It is worth noticing that, almost at the same pressure, two additional broad structures appear as low- and high-frequency shoulders of the $A_g^{(L)}$ and $B_{3g}^{(L)}$ peaks, respectively. These structures, hatched in Fig. 6, were already observed to appear at high pressure (X and Y bands).[20] Their frequencies as a function of pressure,[20] shown in Fig. 3(b) by black and white squares, are in good agreement with our data. These spectral features were ascribed to the onset of a quasiunidimensional ordering in the bc plane,[20] in agreement with some theoretical speculations and experimental findings.[9,26,27]

As mentioned before, the pressure rotates the molecular axis in the bc plane. In particular, in the pressure range explored in the present experiment, the angle γ between the

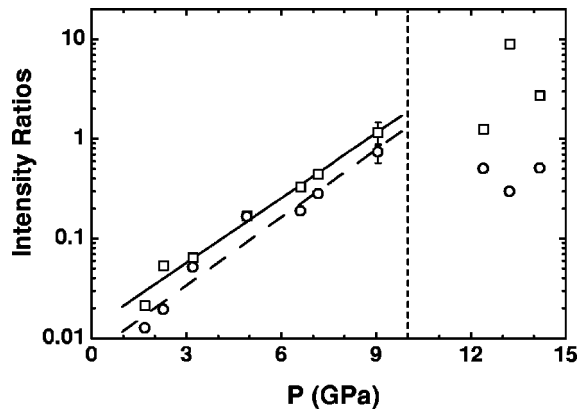

FIG. 5. Integrated intensity ratio between stretching and librational modes as a function of pressure on a logarithmic scale: open squares $A_g^{(L)}/A_g^{(S)}$, open circles $B_{3g}^{(L)}/B_{3g}^{(S)}$. Solid and dashed lines are exponential fitting curves for the A_g and B_{3g} ratios, respectively. The 9 GPa ratios are affected by a large uncertainty since the two stretching peaks are almost superimposed. The dashed vertical line indicates the pressure at which crystal damage occurs.

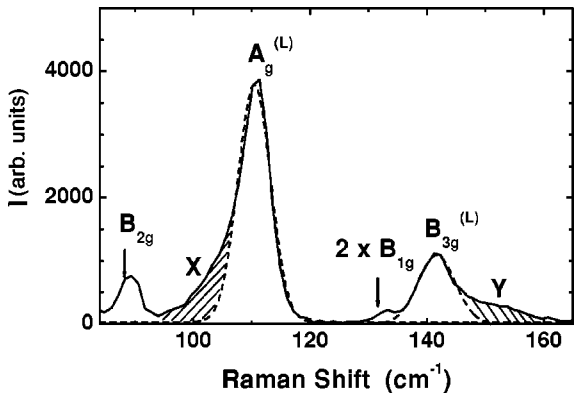

FIG. 6. Raman spectrum of iodine at $P=14$ GPa in the librational frequency region. The new peaks, which appear only above 10 GPa, are marked by arrows (see text). Dotted lines are the best-fit Voigt profiles. The *X* and *Y* structures are indicated by the hatched areas.

molecular axis and the *c* axis increases from 32.2° ($P=0$ GPa) to 37.6° ($P=10$ GPa).[9] As a consequence, on the basis of the simple bond polarizability (BP) model adopted in the previous paper[18] and recognizing that, in the present scattering configuration, the incident electric field makes an angle $\theta>60°$ with the *b* axis, the intensity ratio $A_g^{(S)}/B_{3g}^{(S)}$ is expected to increase with pressure. The large decrease of the $A_g^{(S)}/B_{3g}^{(S)}$ ratio exhibited by our experimental data can only be reproduced by relaxing some of the constraints of the BP model, such as the assumed coincidence between the stretching eigenvector direction and the molecular axis. In particular, if we allow the angle γ', formed by the vibrational stretching eigenvectors with the *c* axis, to differ from the molecular axes angle γ, our results can be interpreted in terms of a reduction of γ' with pressure even if γ is increasing. Indeed very recent theoretical calculations on the pressure evolution of the $A_g^{(S)}$ mode predict a rather large rotation of the $A_g^{(S)}$ eigenvector[16] opposite to the direction of the molecular rotation in the crystal lattice. In particular the value of γ' is predicted to decrease from 27° ($P=0$ GPa) to 5° ($P=10$ GPa), producing a progressive misalignment between the eigenvector and the molecular axes which amounts to 33° at 10 GPa. This effect has been related to pressure-induced rearrangement of the electron density on the *bc* plane, in particular to increases of the nonaxial charge density along the intermolecular charge-transfer bonds. The pressure dependence shown in Fig. 4 is therefore well consistent with the theoretical predictions[16] and can be considered as a clear spectroscopic evidence of a pressure-induced electronic rearrangement. We want to notice that the results reported in our previous paper[18] suggest that the eigenvector is slightly rotated with respect to the molecular axis ($\sim 7°$) also for ambient-pressure iodine, in good agreement with the theoretical estimate.[16]

A second experimental evidence of the pressure-induced electronic rearrangement can be found in the increase of the librational/stretching intensity ratios shown in Fig. 5. At ambient pressure iodine is basically a molecular crystal, the charge being essentially localized within the molecule. In this situation the Raman intensity of the molecular modes is much larger than that of the librational lattice modes ($A_g^{(L)}/A_g^{(S)} \simeq B_{3g}^{(L)}/B_{3g}^{(S)} \leqslant 10^{-2}$ at $P \leqslant 1$ GPa), since the intensity of the latter is due to the molecular polarizability anisotropy and to intermolecular "interaction-induced" polarizability contributions.[28] The present results show that the intensities of the librational modes steeply increase with respect to the intensities of the stretching ones until, in the high-pressure regime, they become almost of the same magnitude ($A_g^{(L)}/A_g^{(S)} \simeq B_{3g}^{(L)}/B_{3g}^{(S)} \simeq 1$ around 10 GPa). This behavior thus indicates that the relevance of intermolecular "interaction-induced" contributions on the Raman spectrum are becoming more and more important with respect to the molecular ones as the density is increased, well consistent with the idea of a progressive charge delocalization outside the molecule over the *bc* plane.[15,22] Moreover, since the intensity ratios increase by more than two orders of magnitude while the *bc* plane surface reduces by less than 15%,[9] the observed effect shows a very strong dependence on the intermolecular distances. Such a behavior suggests the occurrence of considerable "induced" effects[29] due to charge-overlap and charge-transfer mechanisms. The results reported in Fig. 5 can thus be seen as the spectroscopic signature of the onset and of the increased role of the charge-transfer interaction as the pressure is increased. On the other hand, theoretical calculations and advanced x-ray diffraction analysis show that the effect of applying pressure is to strongly enhance nonaxial contributions to the charge density,[18] brought about by the charge-transfer intermolecular bonding. This effect is quite evident in the pressure dependence of the electron density map calculated in Ref. 16 and extracted from x-ray diffraction data in Ref. 15.

It should be noted that, for the A_g modes, pressure-induced electronic rearrangements can in principle also produce variations in the relative strength of the three nonvanishing components of their Raman tensors. A detailed analysis of this effect would require changing the crystal orientation and controlling the polarization of incident and scattered light, both quite difficult tasks using a sample under pressure in a MDAC. Nevertheless, taking into account that the Raman tensors of the B_{3g} modes have only one component (two equal off-diagonal element) the similar pressure behavior shown by the ratios in Fig. 5 suggests that the above mixing effects are not so important, at least as far as the ratio of the A_g modes is concerned.

The appearance of the *X* and *Y* structures in the Raman spectra at pressures greater than 10 GPa also deserves a detailed discussion. Our data confirm the presence of these previously observed structures but in our experiment their appearance seems to be almost simultaneous to that of extra peaks which are forbidden in the adopted sample geometry. Indeed both effects can be understood on the basis of a progressive onset of strong pressure gradients within the sample which can lead to a strong distortion of the peak profile as well as the appearance of forbidden peaks. Also the irregular behavior for the intensity ratios shown in Figs. 4 and 5 above 10 GPa can be ascribed to the presence of anisotropic stresses in the crystal. From our data and in the light of the above discussion the assignment of *X* and *Y* bands to the

onset of zigzag molecular chain structure is therefore doubtful, particularly since this new intermediate phase is not supposed to give rise to any new normal modes.[27]

In conclusion, we have collected room-temperature Raman spectra on iodine single-crystal grown *in situ* on the inner diamond surface of a diamond anvil cell. Spectra have been collected as a function of pressure in the 1–14 GPa pressure range. The quite good quality of the data allows us to perform a careful analysis of the pressure dependence of both internal and external Raman modes. The effect of applying pressure on the sample is that of inducing quite evident modifications in the relative intensities of the four observed Raman-active modes. The pressure behavior found for the $A_g^{(S)}/B_{3g}^{(S)}$ intensity ratio supports the theoretical prediction of a remarkable pressure-induced rotation of the A_g eigenvector in the bc plane and, together with the abrupt increase in the internal to external modes intensity ratio, is in full agreement with a strong displacement of charge density towards intermolecular bonds. This scenario is consistent with the hypothesis of a metallization process brought about by a charge transfer from inside the molecular unit towards the neighbor molecules, along defined directions of charge-transfer bonds.[15,22] Finally the present data show the appearance of several new spectral features for $P>10$ GPa in agreement with previous findings[20] although leaving doubts as to the origin of these structure and to the previously reported interpretation.[20]

[1] H.G. Drickamer, R.W. Lynch, R.L. Clendenen, and E.A. Perez-Albuerne, Solid State Phys. **19**, 135 (1965).

[2] I. Yamamoto, A. Tanaka, and H. Endo, J. Non-Cryst. Solids **156-158**, 728 (1993).

[3] R.S. Mulliken and W.B. Person, *Molecular Complexes* (Wiley, New York, 1969).

[4] U. Buontempo, P. Postorino, and M. Nardone, J. Non-Cryst. Solids **205-207**, 110 (1996).

[5] U. Buontempo, A. Di Cicco, A. Filipponi, M. Nardone, and P. Postorino, J. Chem. Phys. **107**, 5720 (1997).

[6] U. Buontempo, A. Filipponi, P. Postorino, and R. Zaccari, J. Chem. Phys. **108**, 4131 (1998).

[7] F. van Bolhius, P.B. Koster, and T. Migchelsen, Acta Crystallogr. **23**, 90 (1967).

[8] R.M. Ibberson, O. Moze, and C. Petrillo, Mol. Phys. **76**, 395 (1992).

[9] K. Takemura, S. Minomura, O. Shimomura, Y. Fujii, and J.D. Axe, Phys. Rev. B **26**, 998 (1982); H. d'Amour-Sturm and B. Holzapfel, Physica B **139&140**, 328 (1986).

[10] Y. Fujii, K. Hase, Y. Ohishi, N. Hamaya, and A. Ondera, Solid State Commun. **59**, 85 (1986).

[11] Y. Fujii, K. Hase, N. Hamaya, Y. Ohishi, A. Onodera, O. Shimomura, and K. Takemura, Phys. Rev. Lett. **58**, 796 (1987).

[12] R. Reichlin, A.K. McMahan, M. Ross, S. Martin, J. Hu, R.J. Hemley, H.K. Mao, and Y. Wu, Phys. Rev. B **49**, 3725 (1994).

[13] U. Buontempo, A. Filipponi, D. Martinez-Garcia, P. Postorino, M. Mézouar, and J.P. Itié, Phys. Rev. Lett. **80**, 1912 (1998).

[14] P. G. Johannsen, E. F. Dusing, and W. B. Holzapfel, in *Solid State Physics Under Pressure*, edited by S. Minomura (Terra Scientific, Tokyo, 1985), pp. 105–108.

[15] H. Fujihisa, Y. Fujii, K. Takemura, O. Shimomura, R.J. Nelmes, and M.I. McMahon, High Press. Res. **14**, 335 (1995).

[16] K. Yamaguchi and H. Miyagi, Phys. Rev. B **57**, 11 141 (1998).

[17] A. Anderson and T. S Sun, Chem. Phys. Lett. **6**, 611 (1970); B.V. Shanabrook and J.S. Lannin, Solid State Commun. **38**, 49 (1981).

[18] A. Congeduti, M. Nardone, and P. Postorino, Chem. Phys. **256**, 117 (2000).

[19] O. Shimomura, K. Takemura, and K. Aoky, in *High Pressure in Research and Industry*, edited by C. M. Backman, T. Johanisson, and L. Tegner (Uppsala, Arkitektkopia, 1982), p. 272.

[20] H. Olijnyk, W. Li, and A. Wokaun, Phys. Rev. B **50**, 712 (1994).

[21] K. Kobashi and R.D. Etters, J. Chem. Phys. **79**, 3018 (1983).

[22] P.G. Johannsen and W.B. Holzapfel, J. Phys. (Paris), Colloq. **45**, C8-191 (1984).

[23] W. B. Holzapfel, in *High Pressure Science and Technology*, edited by N. V. Novikov and Ye. M. Christyakoo (Naukova Dumka, Kiev, 1989), pp. 120–136.

[24] H.K. Mao, P.M. Bell, J.W. Shaner, and D.J. Steinberg, J. Appl. Phys. **49**, 3276 (1978).

[25] O. Schnepp, J.L. Rosenberg, and M. Goutteran, J. Chem. Phys. **43**, 2767 (1965).

[26] M. Pasternak, J.N. Farrele, and R.D. Taylor, Phys. Rev. Lett. **58**, 575 (1987).

[27] T. Luty and J.C. Raich, Can. J. Chem. **66**, 818 (1988).

[28] D. Frenkel and J.P. McTague, J. Chem. Phys. **72**, 2801 (1980).

[29] D.W. Oxtoby and W.M. Gelbart, Mol. Phys. **29**, 1569 (1975).